

The Manchester occulting mask imager (MOMI) – first results on the environment of P Cygni

J. A. O'Connor, J. Meaburn and M. Bryce

Department of Physics and Astronomy, University of Manchester, Oxford Rd., Manchester, M13 9PL.

Accepted ?? Received ??

ABSTRACT

The design and first use of the Manchester occulting mask imager (MOMI) is described. This device, when combined with the Cassegrain or Ritchey–Chretien foci of large telescopes, is dedicated to the imagery of faint line emission regions around bright central sources.

Initial observations, with MOMI on the Nordic Optical telescope (NOT), of the $V = 4.8$ mag P Cygni environment, have revealed a ≥ 5 arcmin long [N II] $\lambda 6584$ Å emitting filament projecting from the outer nebular shell of this luminous blue variable (LBV) star. The presence of a mono–polar lobe older than both the inner (22 arcsec diameter) and outer (1.6 arcmin diameter) shells is suggested.

Key words: line: profiles – stars: individual: P Cygni – stars: mass-loss – ISM: bubbles.

1 INTRODUCTION

There are a variety of astrophysical problems which require both direct imagery and velocity imagery (i.e. images in small intervals of radial velocity) of faint emission line regions in the close vicinity of dominantly bright sources. For instance, the nebulosities surrounding luminous blue variables (LBVs) are of considerable interest for they are the relics of the most recent eruptions of these stars. Expanding shells of circumstellar gas have now been found around six galactic LBVs (see Barlow et al 1994 and Nota et al 1995 for a summary of these observations). So far, two distinctly different shells have been found (Barlow et al 1994) with occulting–mask imagery around P Cygni ($V = 4.8$ mag). A bright inner shell, ≈ 22 arcsec diameter, has a radial expansion velocity of 140 km s $^{-1}$ in the [N II] $\lambda 6584$ Å line but only 110 km s $^{-1}$ in the exceptionally bright [Ni II] $\lambda\lambda 7378$ & 7412 Å lines. A fainter, outer, [N II] $\lambda 6584$ Å emitting shell of ≈ 1.6 arcmin diameter has been shown to be expanding at 185 km s $^{-1}$ to give a kinematical age of 2100 yr for a distance of 1.8 kpc to P Cygni (Meaburn et al 1996).

The Manchester Echelle spectrometer, MES (Meaburn et al 1984), in its imaging mode, and with an occulting strip in its focal plane, was used for this initial imagery of P Cygni. In this auxiliary mode, MES has a very restricted field–of–view (1.9 arcmin \times 1.5 arcmin) on the Isaac Newton 2.5-m telescope consequently any nebular ejecta from P Cygni of larger angular diameter would remain undetected. The Manchester occulting mask imager (MOMI) has now been manufactured to overcome this restriction. This is a device dedicated to occulting mask imagery and has had

its first use on the Nordic Optical telescope (NOT) where [N II] $\lambda 6584$ Å images of the environs of P Cygni have been obtained over a field area of unprecedented size.

2 OPTICAL LAYOUT OF MOMI

The optical layout of MOMI, at the Ritchey–Chretien focus of the NOT telescope, is shown in Fig. 1. The light is collimated for passage through a narrow–band interference filter, centred on a nebular emission line and placed in the pupil. The field is re–imaged on to the ‘science’ CCD. A pressure stepped, optically contacted, Fabry–Perot etalon can also be included just before the filter in the pupil to permit the option of obtaining spatial/radial velocity data ‘cubes’ of emission line regions around dominantly bright central sources. This option has not yet been used in the present instrument but was built into, and proven astrophysically, in the forerunner (Meaburn & White 1982) of MOMI.

The most critical aspect of the design is that the chromium occulting mask, $\equiv 4$ arcsec on the sky, is on the first surface of the optical chain. With this arrangement, when faint nebulosity around a bright star (e.g. the $V = 4.8$ mag P Cygni) is being imaged, the only contamination of the field is then by the starlight scattered in the atmosphere and reflecting optics of the two–mirror telescope, along with diffraction spikes caused by the spines of the telescope’s secondary mirror mounting. Any refracting optical component prior to this mask floods the field with ‘ghosts’ with such a bright star as a result of multiple reflections. Incidentally, without a mask at all, the contamination by ghosts and scattering of all origins for P Cygni is unnac-

ceable with an integration time of only one second. These contaminations are reduced by tens of thousands of times with the use of the occulting mask.

The optimum size of any mask must depend on the size of the maximum ‘seeing’ disk encountered in one integration yet be small enough not to occult useful information from any circumstellar nebulosity. In this first use, a mask diameter of $\equiv 4$ arcsec was thought to be a good compromise though other possibilities were not explored.

The chromium mask transmits 0.01 percent of the incident light at 6500Å. This is useful in two ways. The position of the star relative to the mask is recorded by the science CCD. Also the stellar position can be monitored throughout the integration by reflecting 8 percent of this light out of the beam with a mylar beamsplitter and forming a broadband image on a secondary CCD, in this case a thermoelectrically cooled Lynx. The transmission of the occulting mask will increase over the 6500Å value by 28 times at 8000Å and decrease by 100 times at 5000Å (Fréedericks 1911).

For the present direct imaging observations at the f/11 Ritchey–Chretien focus of the 2.56-m NOT telescope the 710 mm focal length Tessar collimating lens combined with the 300 mm focal length ‘off-the-shelf’ Nikkor refocussing lens gives a field scale of 1 arcsec = 0.058 mm in the MOMI focal plane. With the thinned Loral 2048 \times 2048 CCD, which has 15 μ m ($\equiv 0.26$ arcsec) square pixels, the field size is 8.83 arcmin \times 8.83 arcmin.

3 OBSERVATIONS AND RESULTS

Narrow band images of P Cygni in the light of [N II] λ 6584 Å were obtained during the night of 1997 November 14 using the Loral CCD as the detector. A three-period (square profile), 20 Å bandwidth, interference filter was centred on the [N II] λ 6584 Å nebular emission line by tilting it by 3.2 deg. Fourteen integrations, each of 500 s duration, were taken with P Cygni centred on the chromium spot.

The data were processed at the University of Manchester STARLINK node with programs from the CCDPACK, FIGARO and KAPPA packages. The data arrays were de-biassed and cosmic ray hits were removed. Flat-field corrections were applied using dusk sky exposures as a reference. The resulting frames were aligned and co-added to give an image with an effective integration time of 7000 s. A star of a similar brightness to P Cygni was also observed in a similar way to permit the correction of the residual scattered stellar continuum from P Cygni.

The full field of MOMI was not used due to a significant drop in quantum efficiency at two adjacent edges of the thinned Loral chip. The occulting spot, which is mechanically offset by a small amount from the centre of the chip, is further offset from the centre of the reduced image when the affected edges are removed from the data array.

A negative, high contrast, grey-scale representation of the trimmed field (8.4 \times 8.4 arcmin²) is shown in Fig. 2. An arc of emission can be seen extending some 5 arcmin from the outer shell towards the North–East of P Cygni. In very deep prints a marginally detected southern counterpart to this 5 arcmin arc can be seen extending directly eastwards from P Cygni.

In Fig. 3 a subsection of the full field array enclosing

the outer shell is shown. Emission extending in the direction of the aforementioned arc is visible. Small bow-shaped knots are apparent in the outer shell at distances 47 arcsec, 48 arcsec, and 52 arcsec to the North–East, South and South–West of the central star respectively. The prominent dark feature to the North–West of the central star is an artefact produced by ghosting within the layers of the interference filter.

A positive grey-scale representation of the inner shell of the P Cygni nebulosity (Barlow et al 1994) is shown in Fig. 4. This is from a subsection of a single data array with only a 500 s integration time. A two dimensional analytical profile, for radii greater than that of the occulting mask and with parameters taken from the continuum reference data (for a star of similar brightness), has been subtracted from the P Cygni data in this image. The central star is seen through the mask. Filamentary loops and arcs within the inner nebular shell, particularly to the North–West of P Cygni, are most striking. Nebular knots are found throughout this shell. Diffraction spikes from the spines of the secondary mirror are broadened due to the field rotation corrector of the altazimuthally mounted NOT. The central spike is due to a fine thread spanning the secondary mirror to secure an alignment cap. Within the full co-added data array the rotation of the altazimuth field causes unacceptable contamination to the image of the inner shell by also rotating the diffraction spikes.

4 DISCUSSION

4.1 Instrumental performance

Narrow-band images of the nebulosity around the bright ($V = 4.8$ mag) star P Cygni have been obtained over a uniquely wide field with MOMI and with better resolution of the small-scale features in the inner and outer nebular shells than has been obtained previously. Furthermore, a faint, extensive, nebular arc has been discovered apparently projecting from these two shells. These observations were made possible by the effectiveness of the chromium occulting mask at limiting the amount of light, from the intense central star, which is transmitted through the refracting optics. Consequently ‘ghosting’ of transmitted starlight from the refractive elements has been reduced to a level that is undetectable in the final image over the whole field.

The present version of MOMI has been designed to be transportable between several telescopes with focal ratios greater than eleven and it has not been optimised for one in particular. Within this limitation, MOMI has performed to design expectations, producing excellent imagery (0.9 arcsec FWHM in 0.7 arcsec seeing) to a field radius of ≈ 4 arcmin. Off-axis optical aberrations in the corners of the field broaden the stellar profiles to ≈ 1.2 arcsec. The Tessar collimator is operating beyond its design limit at the these extreme field angles in a square f/11 field.

Secondary ‘ghosts’ of the brightest parts of the nebulosity which originate within the multi-layers of the interference filter (see Fig. 3) place restrictions on the filters that can be used with this system. All multi-layer, narrow-band interference filters suffer from minor defects in their construction. With careful selection of filters, and with tilt

tuning of the passband position, the filter ‘ghosts’ can be minimised and placed away from areas of interest. The filter ‘ghosts’ could be removed by the subtraction of an image of the same object with the filter tilted by the same amount but in the opposite direction. However, for such a procedure to be successful, when MOMI is combined with an altazimuthally mounted telescope such as the NOT, would also require careful alignment of the diffraction spikes during observations and this was not attempted here.

The processing of data acquired with an equatorially mounted telescope would be far simpler than that obtained with the altazimuthally mounted NOT. For instance, the fixed location of diffraction spikes would facilitate their more complete removal during continuum subtraction. The spikes themselves could also be reduced with the use of a fixed apodising mask in the pupil near the interference filter (see Fig. 1) which is technically more complex to achieve when altazimuth field rotation is involved.

The form of such an apodising mask must be tailored to the individual telescope being used at any given time. The abrupt change in transmission over the narrow widths of the secondary spines must be replaced by graduated changes. A photographically generated apodising mask, fixed in the pupil of an equatorial telescope, should reduce the intensity of the diffraction spikes by a few times. The apodising mask itself would have to rotate during the integration time with respect to the fixed pupil, for an altazimuth telescope, to counter the broadening of the diffraction spikes apparent in Fig. 4.

4.2 P Cygni phenomena

The most striking feature of these initial observations of the environment of P Cygni is the ≥ 5 arcmin long faint nebular arc shown in Fig. 2. This extensive arc appears to be associated with P Cygni and not simply foreground or background nebulosity. It originates at the northern edge of the outer nebular shell, it has a clear connecting filament (see Fig. 3) to the latter and there is a hint of a complementary southern arc, extending nearly west to east from P Cygni. The two arcs could then be the edges of a ‘mono-polar’ lobe projecting from P Cygni. Obviously, the presence of this more southerly arc needs confirming with much deeper imagery and a corresponding western lobe searched for. Single sided nebular lobes, projecting from stars, are unknown whereas bipolar ones are common.

With a distance to P Cygni of 1.8 kpc (Barlow et al 1994) then, if the arc (or lobe) is nearly in the plane of the sky, its linear extent is ≥ 2.6 pc from P Cygni. It is then comparable in dimensions to the extraordinary, faint lobes projecting from the planetary nebula KjPn 8 (López et al 1995). Furthermore, its large angular extent suggests that its formation predates both the 880 yr. age (Barlow et al 1994) of the inner shell in Fig. 4 and the 2100 yr. age (Meaburn et al 1996) of the outer shell in Fig. 3. Measurements of the kinematics of this extensive P Cygni arc/lobe are now required before speculating further about its age and origin.

It is interesting that the optical arc/lobe shown in Fig. 2 appears to have a radio counterpart in the maps of Baars & Wendker (1987) and Skinner et al (1998). As a thermal origin for the radio emission is indicated, radiative ionisation of this extensive feature seems likely.

4.3 Broader use of MOMI

The ionized environments close to a large number of bright stars other than LBVs (e.g. Symbiotics, O & B stars etc.) can be investigated with MOMI in its present form. Additionally, chromium deposited occulting masks can easily be manufactured to prescribed patterns and consequently, MOMI can be used beneficially on a broad range of problems where central sources, of any shape, are extremely bright compared with the adjacent line emission phenomena; e.g. where faint [O III] $\lambda 5007$ Å emitting halos of PNe surround dominantly bright and compact (say 20 arcsec diam.), similarly [O III] $\lambda 5007$ Å emitting, cores. The imagery of the Laques and Vidal (LV) knots (Laques & Vidal 1979) close to the Trapezium group of stars would also benefit if all images of the bright stars in the same field were occulted simultaneously.

The pressure stepped, Fabry–Perot (see Sect. 2) option in the ‘science’ arm (Fig. 1) will have significant application for velocity imagery which also requires an occulting mask. Investigation of the kinematics of the P Cygni shells will require a Fabry–Perot of ‘finesse’ thirty to give a spectral half-width $\equiv 15$ km s $^{-1}$ at an inter-order separation $\equiv 450$ km s $^{-1}$. This whole inter-order range can be covered with the pressure of nitrogen as the scanning gas being increased to 5.36 atmos. above atmospheric pressure. One particular merit of the pressure-stepped Fabry–Perot is its operational simplicity.

5 ACKNOWLEDGEMENTS

JOC and JM acknowledge the excellent assistance of the staff at the Nordic Optical telescope (NOT – La Palma) where these initial observations were made. In particular we are grateful to Hugo Schwartz for his assistance. We thank the technical staff in our department for manufacturing the device and PPARC for funding its construction. JOC also thanks PPARC for a Research Studentship.

6 LEGENDS

Figure 1

The optical layout of MOMI.

Figure 2

The 8.4×8.4 arcmin 2 image of the environs of P Cygni in the light of [N II] $\lambda 6584$ Å.

Figure 3

The outer shell of P Cygni in the light of [N II] $\lambda 6584$ Å. The bright feature to the NW of the star is a ‘ghost’ generated within the layers of the interference filter.

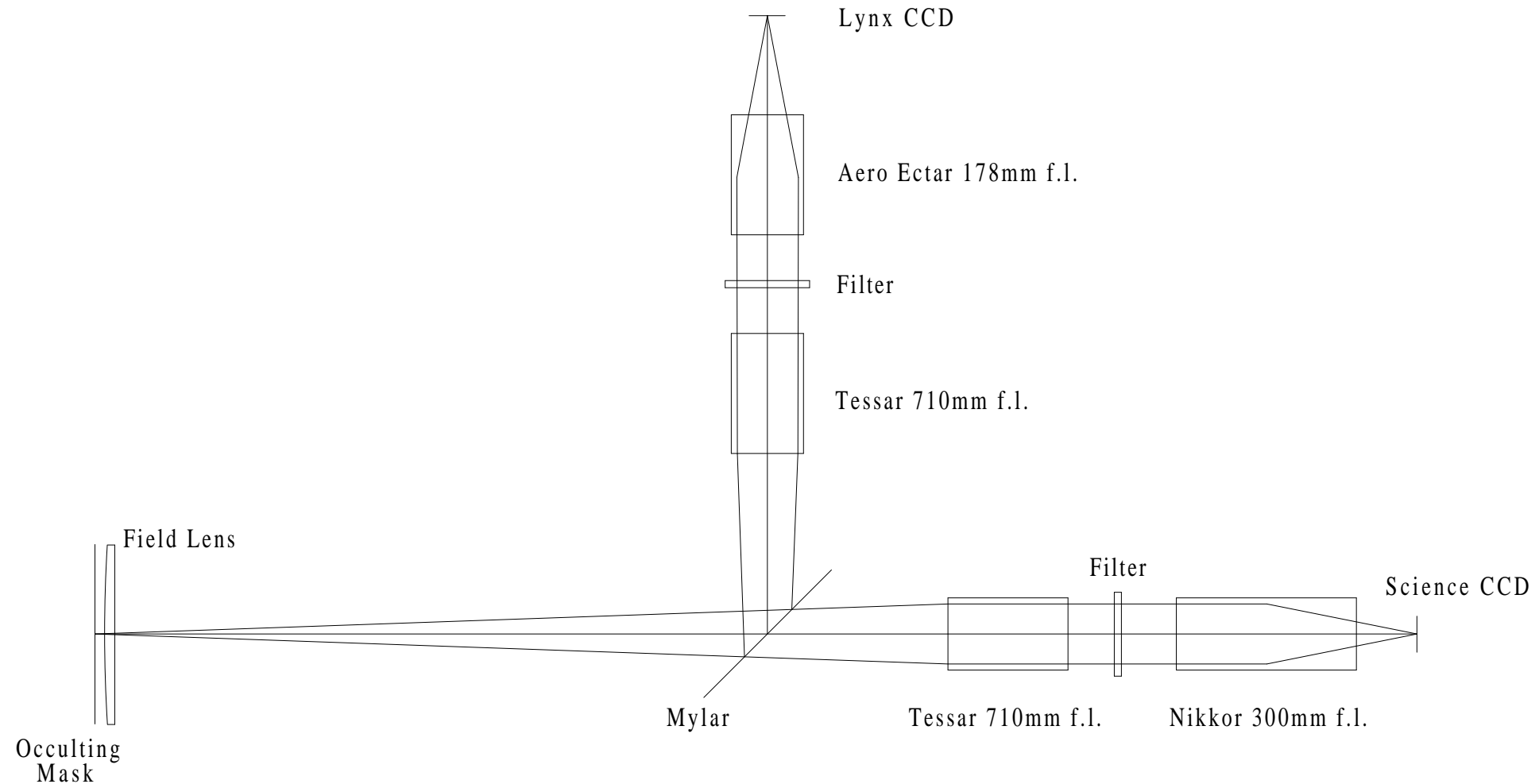
Figure 4

The inner shell in the light of [N II] $\lambda 6584$ Å. The residual scattered stellar continuum has been subtracted by modelling that around a similarly bright star. No attempt has been made to remove the prominent diffraction spikes.

REFERENCES

Baars, J. W. M. & Wendker, H. J., 1987, *A & A*, 181, 210.
 Barlow M. J., Drew J. E., Meaburn J., Massey R. M., 1994, *MNRAS*, 268, L29.
 Fréedericks V., 1911, *Ann. Phys.* [4], 34, 784.
 Lamers H. J. G. L. M., Korevaar P., Cassatella A., 1985, *A&A*, 149, 29.
 Laques, P. & Vidal, J. L., 1979, *A&A*, 73, 97.
 López, J. A., Vázquez, R. & Rodriguez, L. F., 1995, *ApJ*, 455, L63.
 Meaburn, J. & White, N. J., 1982, *Astrophys Space Sci.*, 423 .
 Meaburn J., Blundell B., Carling R., Gregory D. F., Keir D. & Wynne C., 1984, *MNRAS*, 210, 463.
 Meaburn J., López J. A., Barlow M. J. & Drew J. E., 1996, *MNRAS*, 283, L69.
 Nota A., Livio M., Clampin M., Schulte-Ladbeck R., 1995, *ApJ*, 448, 788.
 Skinner, C. J., Becker, R. H., White, R. L., Exter, K. M., Barlow, M. J. & Davis, R. J., 1998, *MNRAS*, in press.

This paper has been produced using the Royal Astronomical Society/Blackwell Science *LATeX* style file.

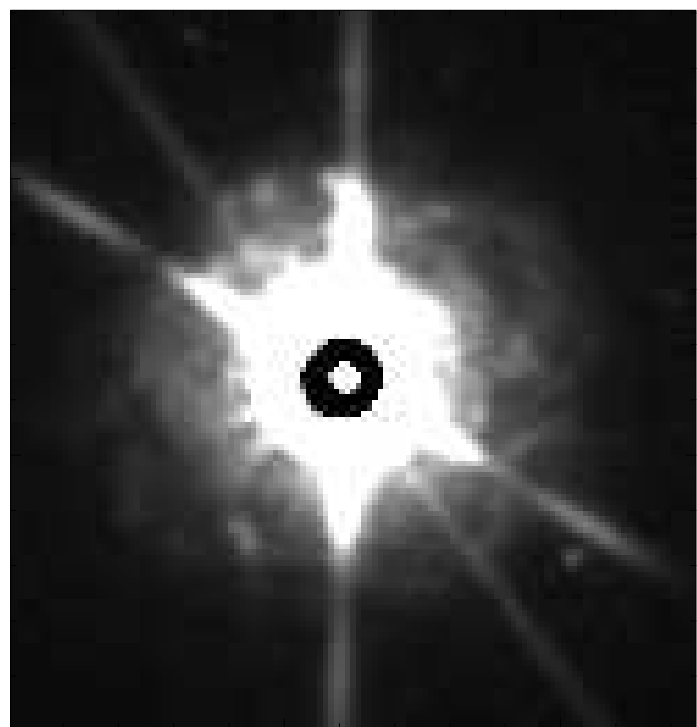


This figure "figure_2.jpg" is available in "jpg" format from:

<http://arxiv.org/ps/astro-ph/9806225v1>

This figure "figure_3.jpg" is available in "jpg" format from:

<http://arxiv.org/ps/astro-ph/9806225v1>



| 10 arcsec |